
Proceedings of the School Superconductivity and Other Phenomena in Perovskites, Warsaw 2004

NMR Study of $(\text{Sr, Ba, La})_2\text{Fe}_{1+y}\text{Mo}_{1-y}\text{O}_6$ Double Perovskites

D. ZAJĄC^{a,*}, CZ. KAPUSTA^a, P.C. RIEDI^b, M. SIKORA^a,
C.J. OATES^a, D. RYBICKI^a, J.M. DE TERESA^c, D. SERRATE^c,
C. MARQUINA^c AND M.R. IBARRA^c

^aDepartment of Solid State Physics, Faculty of Physics and Nuclear Techniques
AGH University of Science and Technology
al. Mickiewicza 30, 30-059 Cracow, Poland

^bDepartment of Physics and Astronomy, University of St. Andrews
St. Andrews, KY16 9SS Scotland, UK

^cInstituto de Ciencia de Materiales de Aragón, Universidad de Zaragoza-CSIC
50009 Zaragoza, Spain

The ⁹⁵Mo and ⁹⁷Mo NMR spin-echo study of $(\text{Sr,Ba,La})_2\text{Fe}_{1+y}\text{Mo}_{1-y}\text{O}_6$ double perovskites is reported. Powder samples of $\text{Ba}_{1.44}\text{Sr}_{0.36}\text{La}_{0.2}\text{FeMoO}_6$ and $(\text{Ba}_{0.8}\text{Sr}_{0.2})_{2-2x}\text{La}_x\#\text{Fe}_{1+y}\text{Mo}_{1-y}\text{O}_6$, where # denotes vacancies, for: $x = 0$, $y = 0$; $x = 0.1$, $x = 0.2$ and $x = 0.3$, $y = 0$ and $y = 0.2$ were measured at 4.2 K and no applied magnetic field. NMR signals are observed at 55–100 MHz for the main line and 30–55 MHz for low-frequency satellite. The main line and the satellite are attributed to the ideal and defect positions of Mo atoms. La and vacancy doping introduce more defects, however, increasing the Fe/Mo ratio decreases the amount of defect Mo sites. La doping causes a satellite pattern at the high frequency side of the spectrum, which is related to different numbers of the La next neighbours. The effect is attributed to an increase in the electron density and the corresponding magnetic moment at the adjacent Mo sites and reveals a local character of the electron doping.

PACS numbers: 75.25.+z, 76.60.-k, 78.70.Gq, 75.47.Gk

1. Introduction

The family of perovskite oxides has recently been a subject of intensive study owing to their extraordinary structural, magnetic, and electronic properties. They

*corresponding author; e-mail: kicaj@uci.agh.edu.pl

reveal a huge decrease in the resistivity in response to an applied magnetic field, which is termed as colossal magnetoresistance (CMR). CMR has been first observed in manganese perovskites. However, their low Curie temperatures, usually below room temperature (RT), resulted in a search for compounds with higher T_C (above room temperature), exhibiting significant magnetoresistance at RT. The examples are Mo–Fe double perovskites, which have a large low-field magnetoresistance at RT [1, 2]. They are known as half-metallic ferrimagnets.

In the ordered double perovskite structure of a general formula $A_2BB'O_6$ (where A is alkaline-earth or rare-earth ion, B and B' are the 3d and 4d or 5d transition metals) the transition element positions are occupied alternately by B and B' cations. The Fe–Mo double perovskites exhibit relatively high magnetic ordering temperatures. Neutron diffraction, X-ray magnetic circular dichroism (XMCD) and nuclear magnetic resonance (NMR) measurements have proven the existence of a non-integer magnetic moment at Mo and Fe sites ([2, 3] and [4]). La substitution was found to increase the Curie temperature and also the number of defects ([5, 6] and [7]). It also increases the Mo hyperfine field value [8]. For the Fe–Mo double perovskite, the ferrimagnetic antiparallel ordering between the Fe and Mo atoms is caused by a double exchange-like interaction (DE) which originates from the t_{2g} spin down electron hopping between $Fe^{2+/3+}$ and $Mo^{6+/5+}$ cations through intervening oxygen antibonding orbitals. This results in a delocalized state of Mo 4d electrons which contribute to the partly filled minority band of the compound [1]. Antisite defects and antiphase boundaries, where the superexchange (SE) interaction of Fe ions dominates, cause a decrease in the magnetization of the sample [9, 10]. The Mo ions at the antisite positions and in antiphase boundaries exhibit weak ferromagnetic interaction through SE [11].

The samples studied in this work were prepared by the solid-state reaction and subsequent annealing at the appropriate temperatures (1200–1500 K) in Ar/H₂ atmosphere. The composition of the polycrystalline powder samples obtained were: $Ba_{1.44}Sr_{0.36}La_{0.2}FeMoO_6$ and $(Ba_{0.8}Sr_{0.2})_{2-2x}La_x\#_xFe_{1+y}Mo_{1-y}O_6$ (where # denotes vacancies), for: ($x = 0$; $y = 0$), ($x = 0.1$, $x = 0.2$ or $x = 0.3$ and $y = 0$ or $y = 0.2$). The barium–strontium ratio, Ba/Sr = 4, and the iron–molybdenum ratio, Fe/Mo = 1 or 1.5 (corresponding to $y = 0$ and 0.2, respectively), are kept constant in series.

In order to determine the influence of doping on the individual atomic site properties the molybdenum NMR experiment has been performed. The measurements were carried out using a frequency swept spin-echo spectrometer [12], at 4.2 K and no applied magnetic field. Powder samples have been measured. The NMR resonant condition is $\omega = \gamma B_e$, where B_e is the effective field at the Mo nucleus and is mainly of the hyperfine interaction origin [3].

2. Results and discussions

The ^{95}Mo and ^{97}Mo NMR spectra normalized to the highest spin-echo signal within individual spectra are shown in Fig. 1. The resonances of both isotopes are unresolved due to their very close gyromagnetic ratios [3]. The base compound $\text{Ba}_{1.6}\text{Sr}_{0.4}\text{FeMoO}_6$ ($x = 0, y = 0$) exhibits a main line at 59.1 MHz and a lower frequency satellite at 43.5 MHz (Fig. 1A), which correspond to the ideal and the defect positions of Mo atoms respectively. Defects include antisite neighbours and antiphase boundaries [11]. From the intensities of the corresponding NMR lines, the content of ideal and defect sites of 86% and 14% is derived, respectively.

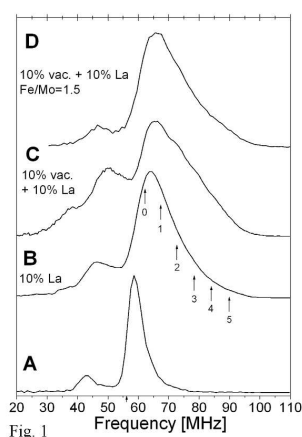


Fig. 1

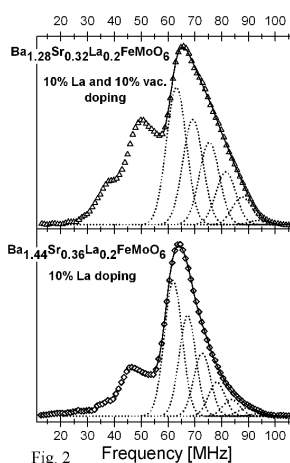


Fig. 2

Fig. 1. ^{95}Mo and ^{97}Mo NMR spectra at 4.2 K and with no external field. For the sample *B*, the satellites corresponding to Mo sites with different numbers of La neighbours are indicated. Samples: *A* — the parent compound — $\text{Ba}_{1.6}\text{Sr}_{0.4}\text{FeMoO}_6$; *B* — $\text{Ba}_{1.44}\text{Sr}_{0.36}\text{La}_{0.2}\text{FeMoO}_6$ — with 10% La doping only, *C* — $\text{Ba}_{1.28}\text{Sr}_{0.32}\text{La}_{0.2}\text{FeMoO}_6$ — with 10% La and 10% vacancies doping, and *D* — $\text{Ba}_{1.28}\text{Sr}_{0.32}\text{La}_{0.2}\text{Fe}_{1.2}\text{Mo}_{0.8}\text{O}_6$ — sample *C* with changed Fe–Mo ratio.

Fig. 2. ^{95}Mo and ^{97}Mo NMR spin-echo spectra at 4.2 K and no applied magnetic field. Dotted lines represent the contributions from the ideal Mo sites with different number of neighbouring La ions (see text). Solid line corresponds to the sum of fitted lines.

Doping with 10% of lanthanum causes a shift of the main line to higher frequencies (61.9 MHz), Fig. 1, comparing with the undoped compound. The intensity of the low frequency satellite increases, which corresponds to an increased amount of defects up to 22% and the centre of gravity of the satellite peak shifts to 46.5 MHz. A poorly resolved satellite pattern appears at the high frequency side of the main line, which corresponds to Mo sites with different La-nearest neighbours. The number of alkaline earth or lanthanum next neighbour sites is 8 [6]. The frequency spacing between neighbouring satellites obtained from the

fit of the spectrum with equidistant Gaussian lines, Fig. 2, is 5.4 MHz. This corresponds to a 2 T increase in the Mo hyperfine field caused by substitution of one alkaline earth ion (Sr or Ba) by one La ion. Using the hyperfine coupling constant for molybdenum of $40 \text{ T}/\mu_B$ [13], similarly to that in [3], an increase in the $4d$ Mo spin moment by $0.05 \mu_B$ per one La neighbour could be derived. The corresponding increase in the number of $4d$ electrons at a Mo site amounts to 0.05 electrons per one La neighbour.

For the sample with 10% La and 10% vacancies, Fig. 1C, the frequency of the main line (the Mo sites with no La neighbours) does not change significantly with hole doping and amounts to 63.5 MHz. The low frequency peak shifts towards higher frequencies (50.4 MHz) and its intensity increases to 34% of the total spectrum. A larger width of the main line compared to the compound with 10% La is observed and the separation of satellites corresponding to different numbers of La neighbours is 6.1 MHz (Fig. 2). The NMR spectrum of the compound $\text{Ba}_{1.28}\text{Sr}_{0.32}\text{La}_{0.2}\text{Fe}_{1.2}\text{Mo}_{0.8}\text{O}_6$, representing 10% La and 10% vacancies as well as Fe/Mo content ratio of 1.5, Fig. 1D, shows the shape and position of the main line similar to that at 10% La and 10% vacancies doping, Fig. 1C. The low frequency peak does not shift but its area decreases compared with the compound having the Fe/Mo content ratio of 1 and amounts to 12% of the total spectrum. This corresponds to the respective decrease in the amount of the Mo defect sites.

A comparison of the compounds with different level of lanthanum and vacancies doping, Fig. 3, shows that the population of defect sites increases with increasing La and vacancies content. A poorly resolved satellite pattern corre-

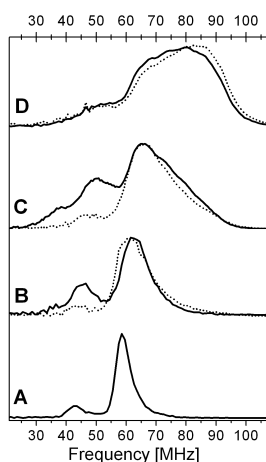


Fig. 3. ^{95}Mo and ^{97}Mo NMR spectra at 4.2 K and without applied magnetic field. Solid line and dotted line correspond to the Fe/Mo ratio equal to 1 and 1.5, respectively. Samples: *A* — the parent compound $\text{Sr}_{0.4}\text{Ba}_{1.6}\text{FeMoO}_6$; *B* — 5% La and 5% vacancies; *C* — 10% La and 10% vacancies, and *D* — 15% La and 15% vacancies.

sponding to the different number of La-nearest neighbours to a molybdenum site is observed for all the compounds, similarly to that in the case of lanthanum doping only. For the compounds with Fe/Mo ratio of 1.5 the intensities of low frequency peaks are smaller than those for Fe/Mo ratio equal to one, which has been attributed to a decreased number of Mo defect sites. However, the Fe excess leads to a considerable amount of Fe antisite ions which couple antiferromagnetically with their neighbours and cause a decrease in bulk magnetization of the compound [7, 10].

The centre of gravity (weighted centre) of the main line and the low frequency satellite shifts towards higher frequencies with La and “hole” doping (Fig. 3). Values of the hyperfine field corresponding to the weighted position of the main line amount to 21.75 T, 23.24 T (23.48 T), 25.64 T (25.35 T), 27.76 T (26.94 T) for $x = 0, 0.1, 0.2, 0.3$ and for Fe/Mo = 1 (Fe/Mo = 1.5), respectively. These values have been used in order to derive the values of the Mo moments at the ideal sites, similarly to that in [3, 13], which amount to $0.54 \mu_B$, $0.58 \mu_B$ ($0.59 \mu_B$), $0.64 \mu_B$ ($0.63 \mu_B$), $0.69 \mu_B$ ($0.67 \mu_B$) for $x = 0, 0.1, 0.2, 0.3$ and for Fe/Mo = 1 (Fe/Mo = 1.5), respectively. In an analogous way, the values of Mo magnetic moments at defect sites were obtained from the hyperfine fields of the low frequency satellite. They amount to: $0.37 \mu_B$, $0.39 \mu_B$ ($0.36 \mu_B$), $0.42 \mu_B$ ($0.38 \mu_B$) and $0.42 \mu_B$ ($0.42 \mu_B$) for $x = 0, 0.1, 0.2, 0.3$ and for Fe/Mo = 1 (Fe/Mo = 1.5), respectively. The values of the Mo magnetic moment are directly related to the $4d$ electron density at the molybdenum site. The tendencies of changes of the electron density at the Mo sites and the corresponding values of the Mo moments at the ideal and defect sites are shown in Fig. 4. The values for the 10% La doped

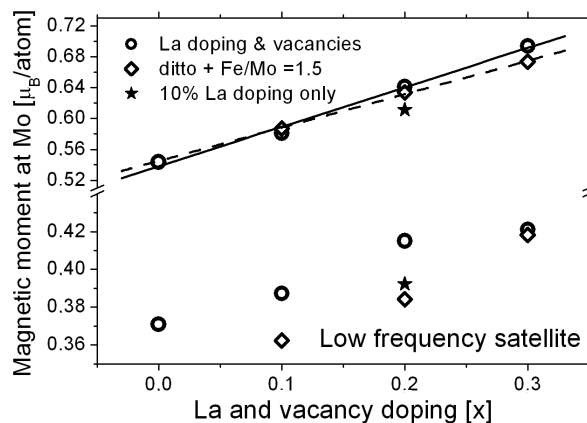


Fig. 4. Molybdenum magnetic moment at the ideal and defect sites as a function of La and vacancies doping (see text). Open circles, open diamonds and filled stars represent samples $(\text{Ba}_{0.8}\text{Sr}_{0.2})_{2-2x}\text{La}_x\#\text{FeMoO}_6$, $(\text{Ba}_{0.8}\text{Sr}_{0.2})_{2-2x}\text{La}_x\#\text{Fe}_{1.2}\text{Mo}_{0.8}\text{O}_6$ and $\text{Ba}_{1.44}\text{Sr}_{0.36}\text{La}_{0.2}\text{FeMoO}_6$, respectively. The solid and dashed lines show the variation of magnetic moment at the ideal Mo sites for the compounds with Fe/Mo = 1 and 1.5, respectively. Magnetic moments have been calculated from weighted centres of lines.

compound compared to that for the 10% La and vacancies doped sample are very similar, which shows that doping with vacancies changes the electron density and the corresponding Mo magnetic moments only slightly.

3. Conclusions

A molybdenum NMR investigation of $(\text{Sr,Ba})_2\text{FeMoO}_6$ double perovskites with La and vacancy doping shows that the observed signal comes from ideal and defect positions of Mo atoms. La and vacancy doping introduce defects, which are observed as the low frequency satellite of the main peak in the NMR spectra. The amount of defect Mo sites decreases with the substitution of Fe for Mo.

La doping creates a satellite pattern at the main line, which corresponds to different number of La neighbours to a Mo site, while vacancies doping bears no influence. The effect corresponds to an increase in the Mo electron density and the corresponding magnetic moment with La doping by $0.05(1) \mu_B$ per one lanthanum neighbour. Doping with vacancies increases the Mo magnetic moment only slightly. The corresponding increase in the number of electrons at the Mo site is 0.05e per one La neighbour. The results show that such an electron doping has a local character. The increase in the electron density and the magnetic moment at the Mo sites results in a higher strength of magnetic interactions between molybdenum and iron. This gives rise to a higher T_C of the lanthanum and vacancies doped compounds.

Acknowledgments

Financial support from the State Committee for Scientific Research (Poland) grant no. 2P03B-08223, the Engineering and Physical Sciences Research Council, UK, and the European Commission, within the RTN SCOOTMO, project no. HPRN-CT-2002-00293 is gratefully acknowledged.

References

- [1] K.-I. Kobayashi, T. Kimura, H. Sawada, K. Terakura, Y. Tokura, *Nature* **395**, 677 (1998).
- [2] C. Ritter, M.R. Ibarra, L. Morellon, J. Blasco, J. Garcia, J.M. De Teresa, *J. Phys. Condens. Matter* **12**, 8295 (2000).
- [3] Cz. Kapusta, P.C. Riedi, D. Zajac, M. Sikora, J.M. De Teresa, L. Morellon, M.R. Ibarra, *J. Magn. Magn. Mater.* **242-245**, 701 (2002).
- [4] M. Besse, V. Cros, A. Barthelemy, H. Jaffres, J. Vogel, F. Petroff, A. Mirone, A. Tagliaferri, P. Bencok, P. Decorse, P. Berthet, Z. Szotek, W.M. Temmerman, S.S. Dhesi, N.B. Brookes, A. Rogalev, A. Fert, *Europhys. Lett.* **60**, 608 (2002).
- [5] J. Navarro, C. Frontera, Ll. Balcells, B. Martinez, J. Fontcuberta, *Phys. Rev. B* **64**, 092411 (2001).

- [6] D. Zając, Cz. Kapusta, P.C. Riedi, M. Sikora, C.J. Oates, D. Rybicki, J. Blasco, D. Serrate, J.M. De Teresa, M.R. Ibarra, *J. Magn. Magn. Mater.* **272-276**, 1756 (2004).
- [7] J. Navarro, J. Nogues, J.S. Munoz, J. Fontcuberta, *Phys. Rev. B* **67**, 174416 (2003).
- [8] M. Wojcik, E. Jedryka, S. Nadolski, J. Navarro, D. Rubi, J. Fontcuberta, *Phys. Rev. B* **69**, 100407(R) (2004).
- [9] W.Y. Lee, H. Han, S.B. Kim, C.S. Kim, B.W. Lee, *J. Magn. Magn. Mater.* **254-255**, 577 (2003).
- [10] J. Linden, M. Karppinen, T. Shimada, Y. Yasukawa, H. Yamauchi, *Phys. Rev. B* **68**, 175515 (2003).
- [11] J.M. Greneche, M. Venkatesan, R. Suryanarayanan, J.M.D. Coey, *Phys. Rev. B* **63**, 174403 (2001).
- [12] J.S. Lord, P.C. Riedi, *Meas. Sci. Technol.* **6**, 149 (1995).
- [13] A. Campbell, *J. Phys. C* **2**, 1338 (1969).